Mapping Formation Pathways and End Group Patterns of Stimuli-Responsive Polymer Systems via High-Resolution Electrospray Ionization Mass Spectrometry

Gene Hart-Smith, Tara M. Lovestead, Thomas P. Davis, Martina H. Stenzel, and Christopher Barner-Kowollik*

Centre for Advanced Macromolecular Design, School of Chemical Sciences and Engineering, The University of New South Wales, Sydney, NSW 2052, Australia

Received March 7, 2007; Revised Manuscript Received May 27, 2007

"Smart" polymers and polymer−protein conjugates find a vast array of biomedical applications. Ambient temperature reversible addition fragmentation chain transfer (RAFT) polymerizations conducted in an aqueous environment are a favorable method of choice for the synthesis of these materials; however, information regarding the initiation mechanisms behind these polymerizations—and thus the critical polymer end groups—is lacking. In the current study, high-resolution soft ionization mass spectrometry techniques were used to map the product species generated during ambient temperature γ-radiation induced RAFT polymerizations of *N*-isopropylacrylamide (NIPAAm) and acrylic acid (AA) in aqueous media, allowing the generated end groups to be unambiguously established. It was found that trithiocarbonate and $^{\bullet}$R radicals produced from the radiolysis of the RAFT agent, $^{\bullet}$OH and $^{\bullet}$OOH radicals produced from the radiolysis of water, and $^{\bullet}$H radicals produced from the radiolysis of water, RAFT agent, or monomer were capable of initiating polymerizations and thus contribute toward the generated chain ends. Additionally, thiol terminated chains were formed via degradation of trithiocarbonate end groups. The current study is the first to provide comprehensive mapping of the formation pathways and end group patterns of stimuli-responsive polymers, thus allowing the design and implementation of these materials to proceed in a more tailored fashion.

Introduction

Stimuli-responsive polymers, also known as "smart" or "intelligent" polymers, undergo dramatic reversible property changes in response to small physical or chemical stimuli; a fact that has allowed these materials to find a vast array of biomedical applications in the delivery of therapeutics, in bioseparations, and in biosensors.[1−5] By conjugating such polymers to proteins, it is possible to create molecular systems for applications such as affinity separations,[6,7] thermoresponsive regulation of enzyme activity,[8] enzyme recovery and recycling,[9] and triggered control of substrate binding to protein active sites.[10,11]

"Living" free radical polymerization protocols have revolutionized the manufacture of well-defined polymers with narrow polydispersities, aiding the construction of these highly specialized biomaterials.[12−14] The recent combination of ^{60}Co γ-radiation with reversible addition and fragmentation chain transfer (RAFT) chemistry[15−24] has opened the avenue for the controlled synthesis of polymers at ambient temperature in an aqueous environment, without the need to incorporate initiator compounds and/or chemical accelerators in the reaction. These nondemanding reaction conditions are ideal for the manufacture of biocompatible polymers, making these polymerization techniques a method of choice for the synthesis of stimuli-responsive polymers[14] and polymer−protein conjugates.[13]

Despite the success of the γ-radiation initiated RAFT process in the construction of "smart" polymers and polymer−protein conjugates, significant gaps in the body of scientific knowledge remain with regards to the mechanistic underpinnings behind these polymerizations as well as the generated end groups. In recent years, some attention has been focused on understanding the mechanisms behind the controlled nature of these systems. Bai et al. suggested that the observed "living" behavior came as a result of a reversible termination mechanism,[15] whereas a conflicting alternative to this reversible termination mechanism was proposed by Quinn et al.[21,22] These authors maintained that the widely accepted mechanism for RAFT polymerizations,[25] as depicted in Scheme 1, was in operation, and they supported this supposition with experiments.[21]

Scheme 1. Basic Mechanism for the RAFT Polymerization Process

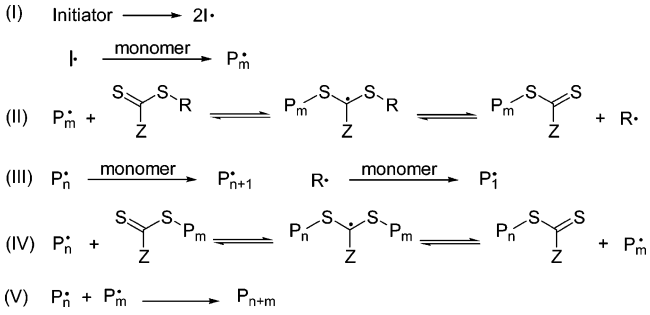

Although the previous kinetic insights into the "living" nature of these systems help in shedding some light on the ambient temperature syntheses of biomaterials via the RAFT technique, details with regards to initiation mechanisms—and thus the critical polymer end groups—are lacking. By conducting pulse radiolysis studies, Acharya et al. found that when γ-radiation is used to produce stimuli-responsive poly(*N*-isopropylacrylamide) (polyNIPAAm), $^{\bullet}$OH and $^{\bullet}$H radicals are capable of acting

* Corresponding author. E-mail: camd@unsw.edu.au or c.barner-kowollik@unsw.edu.au.

10.1021/bm700526j CCC: $37.00
Published on Web 07/26/2007

as initiating species.[26] However, investigations into the initiating capabilities and reactivity of other radicals associated with the radiolysis of species present within these polymerizing systems are sparse.

Mapping the product species produced during these polymerizations using mass spectrometry is a powerful way to investigate the initiating species and hence the initiation mechanisms.[27] The capability of mass spectrometric techniques such as matrix assisted laser desorption and ionization-time-of-flight-mass spectrometry (MALDI-TOF-MS), and electrospray ionization-mass spectrometry (ESI-MS) in the analysis of synthetic polymers has been outlined in numerous publications.[28−34] Although MALDI-TOF-MS is capable of performing analyses over a relatively large mass-to-charge (*m*/*z*) range as compared to ESI-MS (*m*/*z* ≈100 kDa for MALDI-TOF-MS as compared to *m*/*z* <4000 Da for ESI-MS), problems associated with the fragmentation of polymer end groups limit the applicability of this technique.[35−38] On the other hand, ESI-MS is a soft ionization method capable of detecting polymeric products with virtually no chain or end group fragmentation.[27,39−42] Herein, high-resolution state of the art ESI-MS techniques (a Q-TOF Ultima hybrid quadrupole-time-of-flight instrument and a Thermo Finnigan LCQ Deca ion trap mass spectrometer) are employed to arrive at a detailed map of the specific chain ends generated in ambient temperature aqueous system RAFT polymerizations of stimuli-responsive polyNIPAAm and poly(acrylic acid) (polyAA), thereby gaining insight into the mechanistic underpinnings of these polymerizations. The use of such soft ionization methodologies in the current study constitutes an innovative approach toward mapping the end groups of stimuli-responsive polymers and elucidating fundamental radical reactivities in the aqueous ambient temperature RAFT polymerizations used to produce these "smart" materials.

Experimental Procedures

Materials. All chemicals and solvents were purchased from Sigma-Aldrich, Acros, and Fluka at the highest available purity and were used as received unless otherwise noted. NIPAAm was purified by two recrystallizations in *n*-hexane. AA was distilled under vacuum. The synthesis of the RAFT agent *S*,*S*-bis(α,α′-dimethyl-α″-acetic acid)-trithiocarbonate (TRITT) has been described elsewhere.[43] The 300 MHz ^{1}H NMR (DMSO-d_6) analysis of the purified RAFT agent gave δ [ppm] = 1.59 (s, 12H), 12.91 (s, 2H). Careful inspection of the spectrum revealed no impurities.

Polymerization Procedure. γ-Radiation initiated polymerizations of NIPAAm and AA in aqueous media were undertaken using the symmetrical RAFT agent TRITT to mediate the polymerizations. NIPAAm (1.5 mol L^{-1}) or AA (2.5 mol L^{-1}) was dissolved with TRITT in pure water at a monomer/chain transfer agent (CTA) ratio of 200. After the complete dissolution of monomer and RAFT agent, the stock solutions were frozen, placed under vacuum, and re-thawed (repeated 5−10 times) until the solutions were completely deoxygenated. Sealed glass sample vials containing the deoxygenated solutions were placed in an insulated room and exposed to a ^{60}Co source at a dose rate of 0.13 kGy h^{-1}.

Mass Analysis. By identifying the polymeric product ions formed during ESI-MS analyses, detailed maps of the end groups of the stimuli-responsive polymers under study were obtained. These polymeric product ions were identified with the aid of structural libraries created for the possible product species produced in the polymerizing systems under investigation, along with adducts formed from metal cation, salt cluster, and/or solvent molecule attachment to each of these possible product species (see the Results and Discussion for further elaboration). All theoretical molecular weights were calculated using the exact mass as provided by the program package CS ChemDraw 6.0 for the first peak in any given isotopic peak pattern.

Two soft-ionization ESI instruments were employed in the mass spectroscopic studies: a Thermo Finnigan LCQ Deca ion trap mass spectrometer (Thermo Finnigan, San Jose, CA) and a Q-TOF Ultima hybrid quadrupole-time-of-flight instrument (Micromass, Altrincham, Cheshire, U.K.).

The LCQ Deca ion trap instrument was equipped with an atmospheric pressure ionization source operating in the nebulizer assisted electrospray mode and was used in positive ion mode. Mass calibration was performed using caffeine, MRFA, and Ultramark 1621 (Aldrich) in the *m*/*z* range of 195−1822 Da. All spectra were acquired within the *m*/*z* range of 150−2000 Da with spray voltages ranging from 2 to 5 kV, a capillary voltage of 26 V, and a capillary temperature of 275 °C. Nitrogen was used as a sheath gas (flow: 50% of maximum), and helium was used as an auxiliary gas (flow: 5% of maximum). For the analyses of polyNIPAAm, the eluent was a 6:4 v/v mixture of tetrahydrofuran (THF) and methanol with a sodium acetate concentration of 0.1 mM. For the analyses of polyAA, the eluent was a 5:5 v/v mixture of THF and dimethylformamide with a potassium iodide concentration of 0.03 mM. Typical *m*/*z* value errors were observed to be ±0.3 Da. Theoretical isotopic peak patterns were generated using the Xcalibur software.

The Q-TOF instrument was equipped with a ZSpray sample introduction system in a nanoflow electrospray ion source and was used in positive ion mode with a source temperature of 200 °C. Mass calibration was performed using the fragment ions of the Glu-fibrino peptide. Samples were delivered into the ion source from nanospray emitters (Proxeon, Odense, Denmark). The cone voltage offset was set at 35 V, and the system was operated with a capillary voltage of around 800 kV. All spectra were acquired via the TOF analyzer and were integrated every 2.4 s over the *m*/*z* range of 50−2000 Da. Data were recorded and processed using the MassLynx software, version 4.0. For the analyses of polyNIPAAm, the eluent was a 6:4 v/v mixture of tetrahydrofuran (THF) and methanol with a sodium acetate concentration of 0.1 mM. For the analyses of polyAA, the eluent was methanol with a potassium iodide concentration of 0.03 mM. Typical *m*/*z* value errors were observed to be ±0.06 Da. Theoretical isotopic peak patterns were generated using the MassLynx software, version 4.0.

Thermal Stability Studies. PolyNIPAAm was placed in a sealed glass vial, which was immersed in an oil bath heated to 100 °C for 18 h. After the thermal treatment of the polymer sample, mass analysis was performed using the LCQ Deca ion trap instrument.

Results and Discussion

The structural libraries created for the polyNIPAAm and polyAA systems are discussed next, followed by two sections discussing the analyses of ESI-MS spectra generated from polyNIPAAm and polyAA "smart" polymer systems using these structural libraries. The chemical structures assigned to the polyNIPAAm and polyAA systems are summarized within each respective section. A summary of the end group assignments for the stimuli-responsive polymers is then presented, followed by a discussion of the insights gained from the ESI-MS investigations into the fundamental radical reactivities and formation processes involved in these polymerizations.

Structural Libraries. To assign chemical structures to the polyNIPAAm and polyAA systems using ESI-MS, comprehensive structural libraries containing possible polymeric product species were created for each polymer system. During the creation of these libraries, various potential initiating radical species associated with the radiolysis of water, RAFT agent, and monomer compounds were taken into account. These radical species have been summarized in Figure 1.

Scheme 2 shows examples of chemical structures incorporated into the structural libraries. Chemical structures associated with

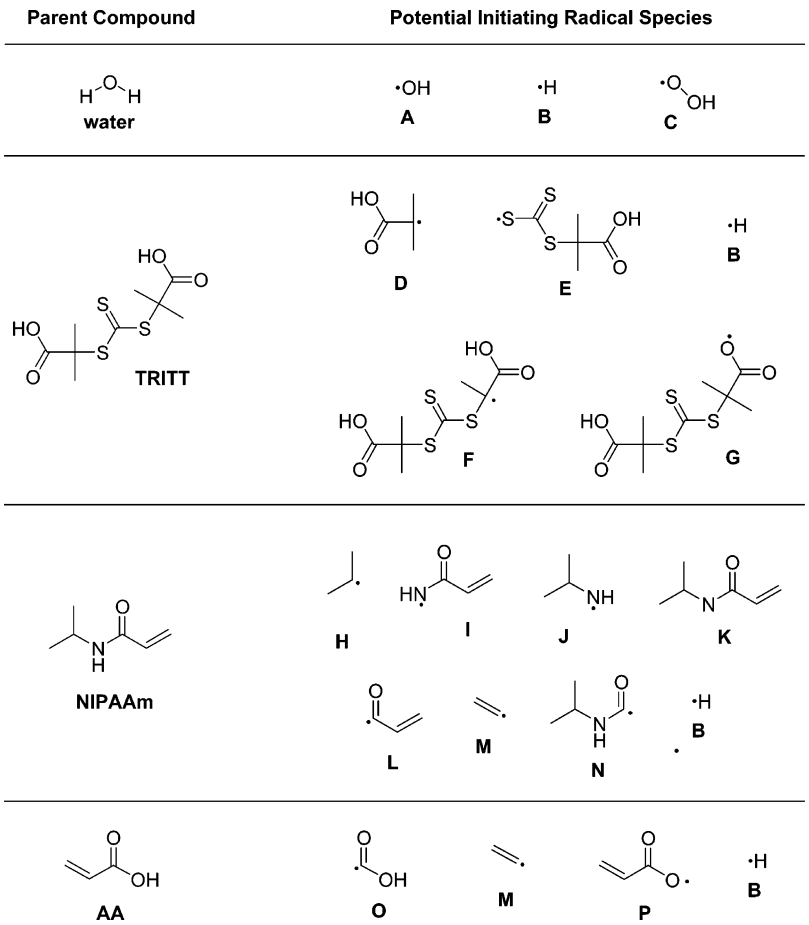

Figure 1. Radicals considered as potential initiating species during the creation of structural libraries for the polyNIPAAm and polyAA polymerizing systems under study. The radicals marked with capital letters are potentially formed from the radiolysis of water,[44,45] TRITT, NIPAAm, or AA.

the widely accepted RAFT mechanism[25] (e.g., structure P_{ED}), including structures that result from either termination via combination (e.g., structure P_{AD}) or termination via disproportionation (e.g., structure D_C), were considered for each potential initiating species listed in Figure 1. In addition, polymer chains containing thiol end groups (e.g., structure P_{ES}), thiolactone end groups (e.g., structure P_{EV}), and disulfide linkages (e.g., structure P_{EWA}), as well as cross-termination products[39,40,46] (see Scheme S1 of the Supporting Information for illustrated examples of cross-termination products), products reinitiated from vinyl end groups, products resulting from chain-transfer to polymer (e.g., structure P_{EAA}), and oxidation products (e.g., structures Ox_1D_{CT} and Ox_2D_{CT}) were also included.

Scheme 2 also shows examples of the nomenclature used when naming the compounds in the structural libraries. This nomenclature is used throughout the present article. Products not immediately identifiable as disproportionation products are named P_{XYZ}, where X and Z correspond to the polymer end groups, and Y corresponds to species present within the polymer chains (where relevant). The X and Z end groups are named following the labeling scheme used to identify the potential initiating species shown in Figure 1. In addition, thiol end groups are labeled with an S, and thiolactone end groups are labeled with a V. For the Y moieties, trithiocarbonate species are labeled with a T, disulfide linkages are labeled with a W, and products resulting from long-chain branching are labeled according to the end group of the branch. Disproportionation products are labeled D_{XY}, following the previous nomenclature. Oxidation products are named Ox_nP_{XYZ} or Ox_nD_{XY}, where n is a number distinguishing one potential oxidation product of species P_{XYZ} or D_{XY} from another. Products that do not fit into any of the aforementioned categories are labeled individually.

For each compound added to a structural library, adduct peaks corresponding to the attachment of various different cations ($[P + n\text{Cat}]^{n+}$, where P represents a polymer molecule, Cat represents sodium, potassium, hydrogen, ammonium, or a solvent molecule, and $n = 1$ for singly charged peaks or $n = 2$ for doubly charged peaks) are considered. When metal salts are added as dopant cations in the ESI-MS experiments, various salt cluster complexes ($[P + M(MX)n]^+$, where MX represents the metal salt, M the metal cation and $n = 1$ or 2) are also taken into account. Exact masses for these adduct species are used to assign peaks in the generated product spectra.

Identification of Products in γ-Radiation Initiated polyNIPAAm. Various experiments were undertaken to confirm the presence of individual polymeric species within the polyNIPAAm system. Complimentary information was obtained from ion trap and Q-TOF mass spectrometry experiments; the thermal stability of the polyNIPAAm system was also investigated, and isotopic peak pattern simulations were performed. The results of each of these investigations are presented next.

Multiple stage mass spectrometry (MS/MS) experiments were also undertaken for the peaks in question in an attempt to distinguish the possible ion assignments from one another. Unfortunately, these experiments yielded little information to differentiate the possible ion assignments, as species of identical mass fragments came off of each of the different ions under the MS/MS conditions employed.

Ion Trap Mass Spectrometry Experiments. The lower portion of Figure 2 shows a product spectrum obtained on the

Scheme 2. Examples of Chemical Structures Incorporated into the Structural Library Created for the TRITT Mediated γ-Radiation Initiated Ambient Temperature Polymerization of NIPAAm in Aqueous Media

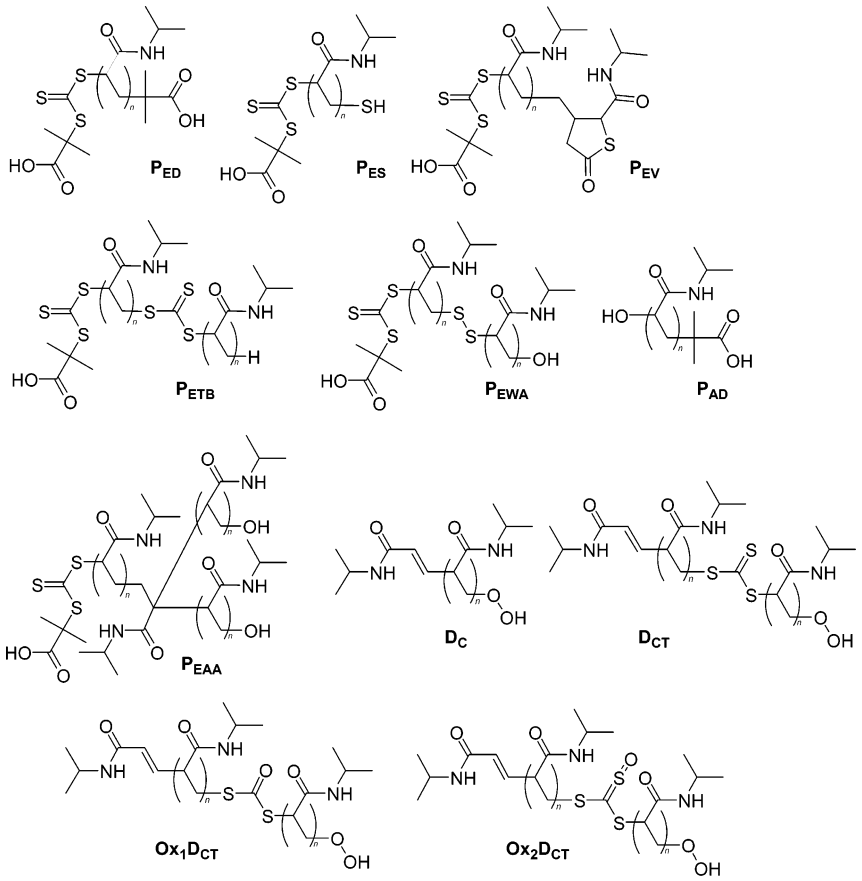

Thermo Finnigan LCQ Deca ion trap mass spectrometer from a sample of TRITT mediated polyNIPAAm produced after exposing the polymerizing system to 60 min of γ-radiation.

The possible ion assignments for the product spectrum shown in Figure 2, based on matching experimental *m*/*z* ratios with the theoretical ratios obtained from the structural libraries, are summarized in Table 1, and the polymeric products identified in γ-radiation initiated polyNIPAAm (based on the final ion assignments as discussed in detail next) have been summarized in Scheme 3.

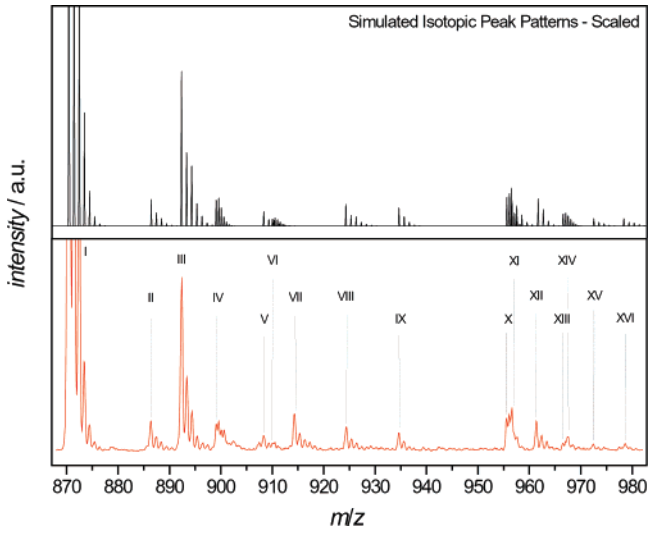

Figure 2. A portion of a mass spectrum obtained on a Thermo Finnigan LCQ Deca ion trap mass spectrometer from a sample of TRITT mediated polyNIPAAm, produced after exposing the polymerizing system to 60 min of ^{60}Co γ-radiation (lower part). All of the peaks that repeat throughout the spectrum are labeled with Roman numerals. Also, simulated isotopic peak patterns for product ion assignments are shown (upper part).

In addition to the products that are unambiguously identified in the polyNIPAAm spectra, adducts formed from various additional chemical structures potentially contribute to the signal intensity of peaks as a result of signal overlap and thus cannot be ruled out as species that are present in the polymer system. The interested reader is referred to Scheme S2 of the Supporting Information for illustrations of these chemical structures.

Careful analyses of the peak assignments listed in Table 1 were undertaken in the process of confirming the previous structural assignments. Of particular concern was the need to distinguish between the various possible ion assignments listed for individual peaks. It can be seen that multiple ion assignments are feasible for peaks I, IV, V, VIII−X, and XII−XVI. An inspection of the chemical nature of the potential product ions helps to determine the feasibility of these different possible ion assignments. For example, as potassium salts were not added to the eluent used in the generation of the previous mass spectrum, it is unlikely that the formation of potassium adducts should take place. For this reason, the potassium adducts assigned to peaks I and V can be disregarded as potential ion assignments. This assumption is further supported by the fact that doubly charged sodium adducts associated with species P_{ED} or P_{DTD} can be attributed to peaks IV and X, which indicate that the product species P_{ED} or P_{DTD} are indeed present in the polymer system. Hence, there is little evidence to suggest that the potassium adducts assigned to peaks I and V contribute toward the signal intensity of the peaks.

Upon further inspection of the potential ion assignments for peak I, it can be seen that the P_{ED} species (illustrated in Scheme

Table 1. Peak Assignments for the Spectrum Obtained from TRITT Mediated PolyNIPAAm Shown in Figure 2[47]

peak	ion assignment(s)	normalized abundance	m/z_{exptl}	m/z_{theor}	error (m/z)
I	$[P_{ED} + Na]^+$	1.00	870.5	870.4	0.1
	$[P_{DTD} + Na]^+$			870.4	0.1
	$[Ox_1P_{ED} + K]^+$			870.4	0.1
	$[Ox_1P_{DTD} + K]^+$			870.4	0.1
II	$[Ox_2P_{ED} + Na]^+$	0.02	886.4	886.4	0.0
	$[Ox_2P_{DTD} + Na]^+$			886.4	0.0
III	$[P_{ETB} + Na]^+$	0.12	892.4	892.3	0.1
IV	$[P_{ED} + 2Na]^{2+}$	0.02	899.1	899.0	0.1
	$[P_{DTD} + 2Na]^{2+}$			899.0	0.1
V	$[P_{ETA} + Na]^+$	0.01	908.3	908.3	0.0
	$[P_{ETB} + K]^+$			908.3	0.0
VI	$[P_{ETB} + 2Na]^{2+}$	0.01	910.2	910.0	0.2
VII	–	0.03	914.3	–	–
VIII	$[P_{ETC} + Na]^+$	0.02	924.4	924.3	0.1
	$[P_{BTB} + Na]^+$			924.5	0.2
	$[P_{ETS} + Na]^+$			924.3	0.1
IX	$[P_{DS} + Na]^+$	0.01	934.6	934.6	0.0
	$[P_{DC} + Na]^+$			934.6	0.0
X	$[P_{ED} + 2Na]^{2+}$	0.02	955.7	955.6	0.1
	$[P_{DTD} + 2Na]^{2+}$			955.6	0.1
XI	$[P_{STB} + Na]^+$	0.03	956.6	956.5	0.1
	$[P_{ATA} + Na]^+$			956.5	0.1
XII	$[P_{AA} + Na]^+$	0.02	961.4	961.7	0.3
	$[P_{BC} + Na]^+$			961.7	0.3
	$[P_{BS} + Na]^+$			961.6	0.2
XIII	$[Ox_1P_{ED} + Na]^+$	0.01	967.5	967.5	0.0
	$[Ox_1P_{DTD} + Na]^+$			967.5	0.0
XIV	$[P_{ETB} + 2Na]^{2+}$	0.01	966.5	966.5	0.0
XV	$[P_{ATC} + Na]^+$	0.01	972.5	972.5	0.0
	$[P_{ATS} + Na]^+$			972.5	0.0
XVI	$[P_{AC} + Na]^+$	0.01	977.5	977.6	0.1
	$[P_{AS} + Na]^+$			977.6	0.1

3) associated with the peak is the main product expected to be formed from the widely accepted RAFT mechanism. Product ions similar to the adducts potentially formed from species P_{ED} have been reported as the most abundant ions observed in past mass spectrometry studies.[39−41] As peak I displays the highest signal intensity of the product peaks observed in the mass spectrum, this suggests that peak I can be attributed predominantly, if not entirely, to ions formed from the P_{ED} species. It follows that peaks IV and X also can be attributed predominantly, if not entirely, to ions formed from these species and that peaks II and XIII likely appear as a result of ions formed from oxidized versions of species P_{ED}.

Ions formed from polymeric species with thiol end groups are listed as possible assignments. The observation of thiol terminated chains has been reported in previous mass spectrometry studies,[40,48] and Llauro et al. attributed the observation of these thiol terminated species to the cleavage of trithiocarbonate moieties present in polymer chains.[48] For the thiol terminated polymer chains that are listed as potential adduct assignments (P_{DS}, P_{BS}, P_{SS}, P_{ETS}, P_{STB}, and P_{ATS}), all but species P_{ETS} can conceivably form via the cleavage of trithiocarbonate containing polymer chains that also can be assigned to peaks as adduct species (P_{ED}, P_{ETC}, P_{BC}, P_{DTD}, P_{ETB}, P_{BTB}, P_{ATA}, P_{ATC}, and P_{ETA}). For species P_{ETS}, no ions associated with parent molecules capable of degrading into this particular thiol terminated chain are able to be assigned to any of the observed peaks (see Scheme 4). Similarities in end group functionality suggest that it is unlikely that any parent molecules required for the formation of the P_{ETS} species would ionize to a significantly lesser degree than the parent molecules required for the formation of the other thiol terminated chains in question. Hence, the fact that adducts associated with the required parent species are not observed strongly suggests that these species are indeed not present within the polymer system in question. Therefore, the $[P_{ETS} + Na]^+$ adduct is excluded as a possible ion assignment for peak VIII with a considerable degree of confidence.

Thermal Stability Studies. As an added means of investigating whether or not several of the product peaks observed in the previous ion trap spectrum arise as a result of thiol terminated chains formed via the degradation of trithiocarbonate end groups, a hypothesized thermal degradation mechanism relating to these polymeric species was examined (as shown in Scheme 5). To undertake these studies, spectra produced from polyNIPAAm before and after thermal treatment were compared. The upper portion of Figure 3 shows an ion trap spectrum obtained from the thermally treated polymer sample, covering a m/z range identical to the spectrum obtained from the polymer sample prior to thermal treatment (shown in the lower portion of Figure 3). Relative peak intensities were compared before and after the thermal treatment of the polymer sample (Table 2).

The previous results strongly support the hypothesized formation of thiol terminated chains via the thermal degradation of structures containing trithiocarbonate end groups. Inspection of the spectra before and after heat treatment reveals significant changes in signal intensity for peaks I−VI, VIII−XI, XIII, and XIV. Additional peaks not observed in the original mass spectrum are also present in the heated sample, designated as peaks IVa, XVII, and XVIII. Several of these peaks can immediately be identified as unimportant when discussing the proposed thermal degradation mechanism. For instance, the lack of multiple charging observed in the spectrum obtained from the heated sample accounts for the complete disappearance of peaks IV, VI, X, and XIV. Additionally, peaks II and XIII are due to adducts formed from the oxidation of species P_{ED} from peroxides present in the solvent used in the mass spectrometry studies, and the significant changes in signal intensity of these peaks is ascribed to the differing times in which the sample solutions were stored prior to analysis.

Of the remaining peaks in question, the most important of these peaks (in terms of the hypothesized thermal degradation) have been listed in Scheme 5 alongside illustrations of structures associated with these peaks. The only peaks in the original product spectrum that are assigned unambiguously as singly charged adducts formed from trithiocarbonate containing species are peaks I, III, and V (from the trithiocarbonate containing species P_{ED}, P_{ETB}, and P_{ETA} respectively); hence, it would be expected that thermal degradation of these species would result in a decrease in signal intensity for these peaks. A trithiocarbonate structure similar to these unambiguously assigned molecules (that is, species P_{ETC}) may also be a structure capable of producing the ions observed as peak VIII in the original mass spectrum (see Figure 2). Hence, if the thermal treatment of the polymer sample did in fact result in the degradation of the trithiocarbonate containing structures, this peak would decrease in signal intensity if structure P_{ETC} indeed does exist. In addition, the degradation of trithiocarbonate end groups from structures P_{ED}, P_{ETB}, P_{ETA}, and P_{ETC} should result in the formation of the thiol terminated species P_{DS}, P_{STB}, P_{ATS}, and P_{STC}, respectively. Any additional sodium adducts formed from species P_{DS}, P_{STB}, and P_{ATS} would produce an increase in the signal intensities of peaks IX, XI, and XV, respectively, and sodium adducts formed

Scheme 3. Polymeric Products Identified in Spectra Produced from TRITT Mediated PolyNIPAAm Initiated via γ-Radiation in Aqueous Media

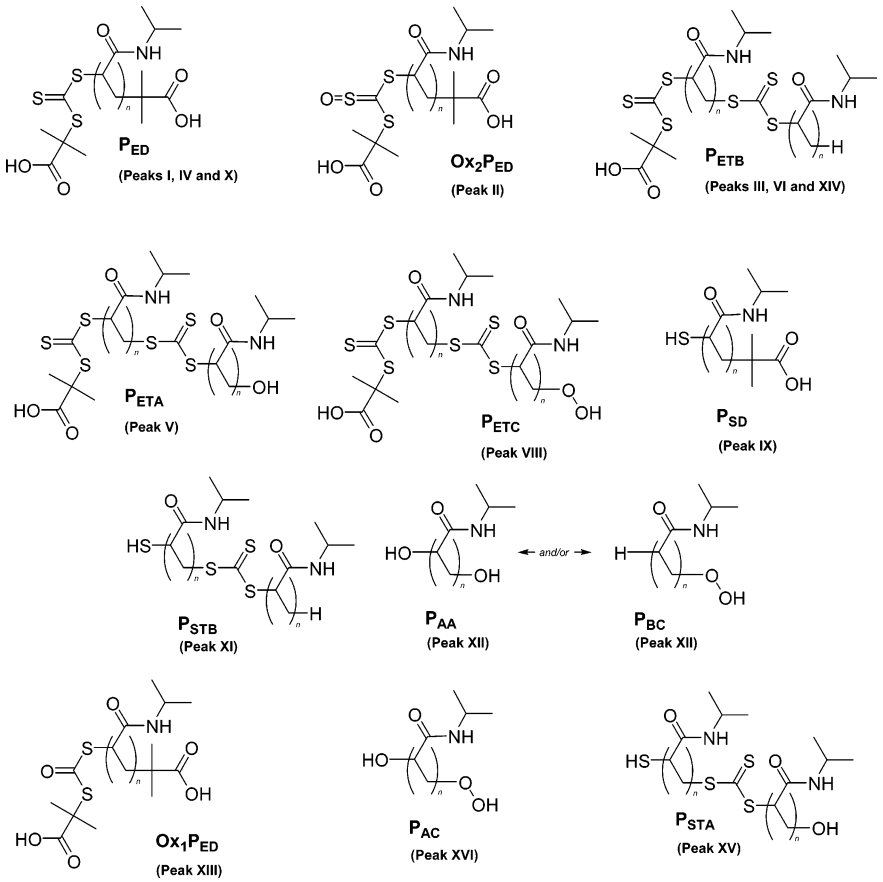

Scheme 4. Hypothetical Formation of Species P_{ETS} via Trithiocarbonate End Group Degradation of Its Parent Molecule, Species P_{ETE}[a]

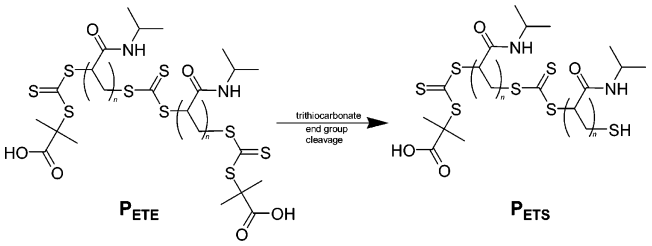

[a] Absence of species P_{ETE} in the polymer system also indicates the absence of species P_{ETS}.

from species P_{STC} would produce a previously unobserved peak at a *m*/*z* ratio of 875.4 (peak XVII). As shown in Table 2 and Scheme 5, peaks I, III, V, and VIII do decrease appreciably in signal intensity. Additionally, peaks IX and XI increase appreciably in signal intensity. Peak XV also increases in intensity; however, this increase is below the range of experimental error and alone is not significant. Of particular interest, the predicted peak XVII is observed in the spectrum produced from the heated sample, strongly supporting the hypothesis that the trithiocarbonate end groups of species P_{ED} and P_{ETB} degrade to form the thiol terminated chains P_{DS} and P_{STB}. Also, species P_{ETA} is assumed to degrade in a similar manner to form the thiol terminated chain P_{ATS}, and the relatively low intensity of peak XV in the spectrum obtained from the heated sample stems from the originally minor abundance of the parent P_{ETA} species. The appearance of peak XVII coupled with the decrease in the signal intensity of peak VIII lends solid support to the supposition that the P_{ETC} species degrades to form the thiol terminated species P_{STC}. From the previous evidence, the thiol terminated species P_{DS}, P_{STB}, and P_{ATS} are assumed to exist in the polymer system as a result of the degradation of polymer chains with trithiocarbonate end groups. Additionally, the ion assignments for peaks IX, XI, and XV can, at least in part, be ascribed confidently to the $[P_{DS} + Na]^+$, $[P_{STB} + Na]^+$, and $[P_{ATS} + Na]^+$ adducts, respectively. Lastly, the evidence for degradation of species P_{ETC} suggests that this species is indeed present in the polymer system and that peak VIII can, at least in part, confidently be ascribed to the $[P_{ETC} + Na]^+$ adduct.

In addition to the observed cleavage of trithiocarbonate end groups, thermal cleavage of the trithiocarbonate moiety present within the chain centers of species P_{ETB}, P_{ETA}, and P_{ETC} may occur theoretically, resulting in the formation of structures P_{BS}, P_{AS}, P_{CS}, and P_{SS}. Under such a scenario, ions formed from these thiol terminated species would produce an increase in the signal intensities of peaks XII and XVI, and a previously unobserved peak with a *m*/*z* ratio of 880.5 would be expected in the spectrum produced from the heated sample. The fact that none of these indicators is detected suggests that the cleavage of trithiocarbonate moieties present within the chains of species P_{ETB}, P_{ETA}, and P_{ETC} does not occur and that the species P_{BS}, P_{AS}, P_{CS}, and P_{SS} are not formed during the polymerization. Therefore, the adducts $[P_{BS} + Na]^+$ and $[P_{AS} + Na]^+$ are confidently excluded as possible ion assignments for peaks XII and XVI, respectively.

Q-TOF Mass Spectrometry Experiments. To help confirm the presence of the structures observed in the ion trap mass spectrometry experiments, complimentary data were generated by undertaking Q-TOF mass spectrometry experiments. Product peaks corresponding to the $[P_{ED} + Na]^+$ and $[P_{ED} + 2Na]^{2+}$ ions previously assigned to peaks I, IV, and X, respectively, in

Scheme 5. Hypothesized Thermal Degradation of Structures Containing Trithiocarbonate End Groups, Resulting in the Formation of Thiol Terminated Chains[a]

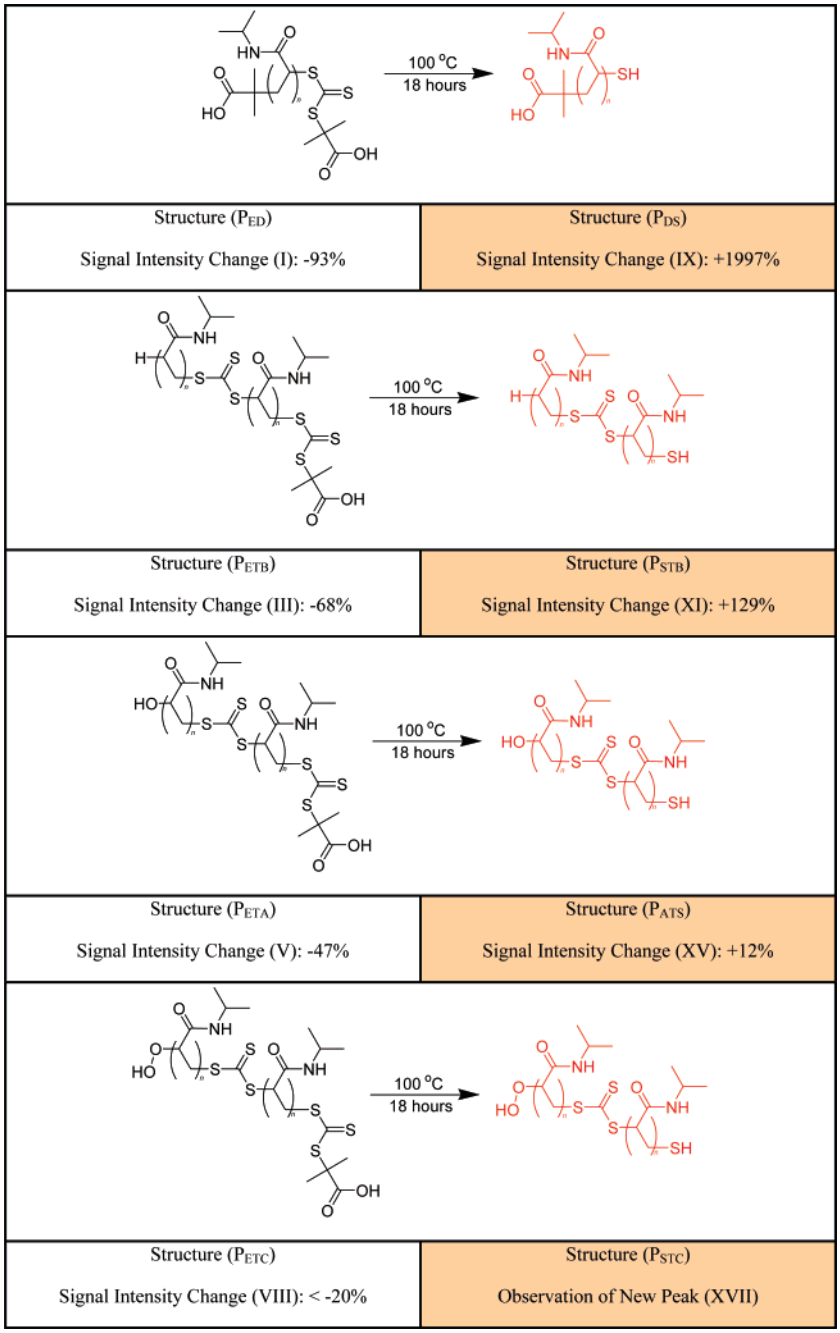

[a] Product peaks associated with sodium adducts potentially formed from these structures are listed, along with the observed changes in signal intensity for each of these peaks in the spectrum obtained from a thermally treated polymer sample, relative to the spectrum obtained from an unheated polymer sample.

the spectrum obtained from the ion trap mass spectrometer are accurate to within 0.01 Da in spectra produced from the Q-TOF mass spectrometer when an external calibration is used. In addition, simulated isotopic peak patterns for these adduct species show excellent agreement with the experimentally obtained isotopic peak patterns. These observations serve to confirm the ion assignments for peaks I, IV, and X. The interested reader is referred to Figure S1 of the Supporting Information for complete illustrations of these experiments.

Isotopic Peak Pattern Simulations. As a final aid to confirm the presence of the structures assigned to the polymer system in the previous mass spectrometry experiments, isotopic peak pattern simulations were undertaken. Isotopic peak pattern simulations are useful to aid in confirming potential ion assignments, especially in cases when multiple ion assignments are possible for a product peak. This is possible when the different ion assignments have different chemical formulas and/or the experimentally obtained isotopic peak patterns are clearly resolved without peak overlap occurring. Such simulations suggest that peak VIII of the ion trap spectrum arises predominantly due to the $[P_{ETC} + Na]^+$ adduct, whereas for peaks IX, XII, and XV, the presence of the different adduct species assigned to the peaks is equally likely. The interested reader is referred to Figure S2 of the Supporting Information for complete illustrations of the simulations.

The scaled isotopic peak pattern simulations for the final ion assignments are shown in the upper portion of Figure 2.

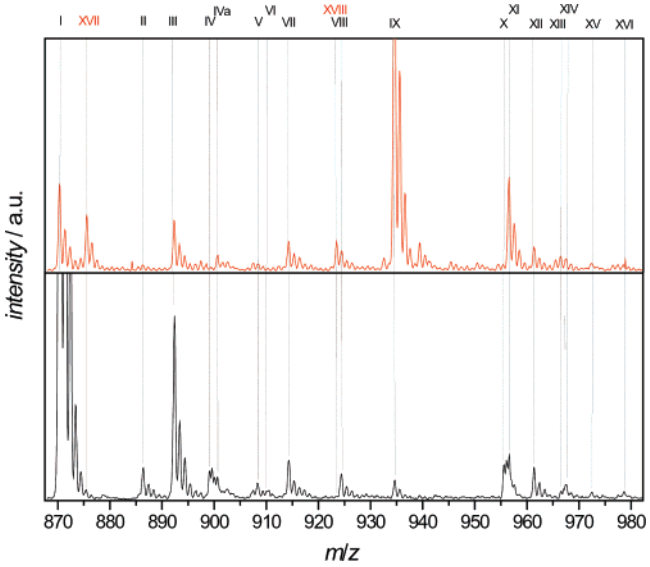

Figure 3. Portion of a spectrum obtained on a Thermo Finnigan LCQ Deca ion trap mass spectrometer from the sample of TRITT mediated polyNIPAAm used to produce the spectrum illustrated in Figure 2, after the sample had been heated at 100 °C for 18 h (upper part), along with the spectrum obtained from the sample prior to thermal treatment, shown over the same *m*/*z* and intensity ranges (lower part). The signal intensities for the spectrum obtained from the heated polymer sample were corrected to take into account the differing signal intensities observed in neat solvent spectra prior to analyzing the respective heated and unheated samples.

Excellent agreement is observed between the simulated results and the results obtained experimentally from the ion trap instrument.

Identification of Products in γ-Radiation Initiated polyAA. As with the identification of the product species in γ-radiation initiated polyNIPAAm, various experiments were undertaken to confirm the presence of polymeric species within the polyAA system under study. Complimentary information was obtained from ion trap and Q-TOF mass spectrometry experiments, and isotopic peak pattern simulations were performed.

Ion Trap Mass Spectrometry Experiments. The lower portion of Figure 4 shows a product spectrum obtained on a Thermo Finnigan LCQ Deca ion trap mass spectrometer from a sample of TRITT mediated polyAA produced after exposing the polymerizing system to 120 min of γ-radiation.

The possible ion assignments generated for the product spectrum shown in Figure 4, based on matching theoretical and experimental *m*/*z* ratios, are summarized in Table 3, and the polymeric products identified in γ-radiation initiated polyAA (based on the final ion assignments as discussed in detail next) are summarized in Scheme 6.

In a similar manner to the polyNIPAAm system, adducts formed from various additional chemical structures potentially contribute to the signal intensity of peaks observed in spectra produced from polyAA as a result of signal overlap, and thus cannot be ruled out as species that are present in the polymer system. The interested reader is referred to Scheme S3 of the Supporting Information for illustrations of these chemical structures.

Once again, to distinguish between the various possible ion assignments listed for individual peaks, careful analyses of the listed peak assignments (Table 3) were undertaken in the process of confirming the previous structural assignments. It can be seen that multiple ion assignments are feasible for peaks I−III, V, VI, and IX−XI. As with the polyNIPAAm system, an inspection

Table 2. Signal Intensities for Peaks I−XVI in TRITT Mediated PolyNIPAAm Spectra before and after Heat Treatment[49]

peak	ion assignment(s)	intensity before heat treatment (a.u.)	corrected intensity after heat treatment (a.u.)	% change (±20)
I	$[P_{ED} + Na]^+$ $[P_{DTD} + Na]^+$ $[Ox_1P_{ED} + K]^+$ $[Ox_1P_{DTD} + K]^+$	4.5×10^6	3.0×10^5	−93
II	$[Ox_2P_{ED} + Na]^+$ $[Ox_2P_{DTD} + Na]^+$	9.8×10^4	2.2×10^4	−78
III	$[P_{ETB} + Na]^+$	5.6×10^5	1.8×10^5	−68
IV	$[P_{ED} + 2Na]^{2+}$ $[P_{DTD} + 2Na]^{2+}$	8.9×10^4	0	−100
IVa	–	–	5.7×10^4	–
V	$[P_{ETA} + Na]^+$ $[P_{ETB} + K]^+$	5.5×10^4	2.9×10^4	−47
VI	$[P_{ETB} + 2Na]^{2+}$	2.8×10^4	0	−100
VII		1.2×10^5	1.0×10^5	−17
VIII	$[P_{ETC} + Na]^+$ $[P_{BTB} + Na]^+$ $[P_{ETS} + Na]^+$	8.4×10^4	$<6.7 \times 10^4$	<−20
IX	$[P_{DS} + Na]^+$ $[P_{DC} + Na]^+$	6.2×10^4	1.3×10^6	+1997
X	$[P_{ED} + 2Na]^{2+}$ $[P_{DTD} + 2Na]^{2+}$	1.1×10^5	0	−100
XI	$[P_{BC} + Na]^+$ $[P_{STB} + Na]^+$ $[P_{ATA} + Na]^+$ $[P_{AA} + Na]^+$	1.4×10^5	3.2×10^5	+129
XII	$[P_{BC} + Na]^+$ $[P_{BS} + Na]^+$	9.9×10^4	8.4×10^4	−15
XIII	$[Ox_1P_{ED} + Na]^+$ $[Ox_1P_{DTD} + Na]^+$	3.0×10^4	3.8×10^4	+27
XIV	$[P_{ETB} + 2Na]^{2+}$	3.5×10^4	0	−100
XV	$[P_{ATC} + Na]^+$ $[P_{ATS} + Na]^+$	2.6×10^4	2.9×10^4	+12
XVI	$[P_{AC} + Na]^+$ $[P_{AS} + Na]^+$	2.7×10^4	2.4×10^4	−11
XVII	$[P_{STC} + Na]^+$	0	1.9×10^5	–
XVIII	–	0	1.0×10^5	–

of the chemical nature of the potential product ions helps to determine the feasibility of these different assignments when multiple ion assignments are possible. As mentioned previously, unambiguous observations of high abundances of adducts formed from species similar to P_{ED} have been reported previously in mass spectrometry studies,[39−41] suggesting that peak I can be attributed predominantly, if not entirely, to $[P_{ED} + K]^+$ ions. Additionally, ion assignments associated with the parent molecules required for the formation of the thiol terminated species P_{ETS} are not possible for any of the observed peaks. Therefore, the $[P_{ETS} + K]^+$ adduct is excluded as a possible ion assignment for peak IX for the same reasons that the similar $[P_{ETS} + Na]^+$ adduct was excluded as an ion assignment in the TRITT mediated polyNIPAAm system.

Q-TOF Mass Spectrometry Experiments. As with the experiments conducted upon polyNIPAAm, complimentary data were generated for the polyAA system by undertaking Q-TOF mass spectrometry experiments. Figure 5 displays a spectrum obtained from TRITT mediated polyAA using the Q-TOF instrument. Peak assignments for the product spectrum shown in Figure 5, based on matching theoretical and experimental *m*/*z* ratios, are summarized in Table 4.

Inspection of the ion assignments listed for the displayed Q-TOF spectrum reveals that singly charged sodium and potassium adduct peaks as well as doubly charged sodium adduct peaks associated with species P_{ED} are observed. In addition, the spectrum further confirms the presence of species P_{ETA} and P_{ETB}, observed as doubly charged sodium and potassium adducts, respectively.

Importantly, peak C is associated with doubly charged potassium adducts formed from at least one of the species

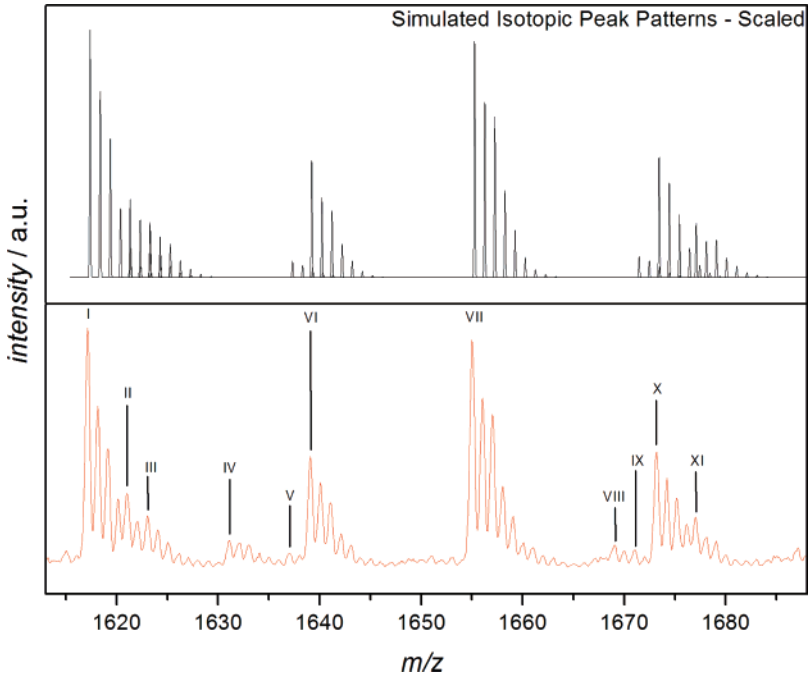

Figure 4. A portion of a mass spectrum obtained on a Thermo Finnigan LCQ Deca ion trap mass spectrometer from a sample of TRITT mediated polyAA, produced after exposing the polymerizing system to 120 min of ^{60}Co γ-radiation (lower part). All of the consistently repeating peaks throughout the spectrum are labeled with Roman numerals. Also, simulated isotopic peak patterns for product ion assignments are shown (upper part).

Table 3. Peak Assignments for the Spectrum Obtained from TRITT Mediated AA Shown in Figure 4[50]

peak	ion assignment	normalized abundance	m/z_{exptl}	m/z_{theor}	error (m/z)
I	$[P_{ED} + K]^+$	1.0	1617.2	1617.3	0.1
	$[P_{DTD} + K]^+$			1617.3	0.1
	$[P_{BTC} + K]^+$			1621.3	0.3
II	$[P_{STB} + K]^+$	0.32	1621.0	1621.3	0.3
	$[P_{ATA} + K]^+$			1621.3	0.3
III	$[P_{ETB} + Na]^+$	0.22	1623.0	1623.3	0.3
IV	–	0.12	1631.1	–	–
V	$[P_{ATC} + K]^+$	0.07	1637.0	1637.3	0.3
	$[P_{ATS} + K]^+$			1637.3	0.3
	$[P_{ETA} + Na]^+$			1639.2	0.1
VI	$[P_{ED} + K(KI)]^+$	0.47	1639.1	1639.2	0.1
	$[P_{ETB} + K]^+$			1639.2	0.1
VII	$[P_{ETA} + K]^+$	0.95	1655.1	1655.2	0.1
VIII	–	0.10	1669.1	–	–
IX	$[P_{DS} + K]^+$	0.09	1671.1	1671.4	0.3
	$[P_{DC} + K]^+$			1671.4	0.3
	$[P_{ETC} + K]^+$			1671.2	0.2
	$[P_{ETS} + K]^+$			1671.2	0.2
	$[P_{ED} + Na]^+$			1673.4	0.2
	$[Ox_1P_{ED} + K]^+$			1673.4	0.2
X	$[P_{AS} + K]^+$	0.49	1673.2	1673.4	0.2
	$[P_{AC} + K]^+$			1673.4	0.2
	$[P_{CS} + Na]^+$			1673.4	0.2
XI	$[P_{ETA} + K(KI)]^+$	0.22	1677.0	1677.0	0.0
	$[P_{AE} + Na]^+$			1677.3	0.3

Ox_1P_{ED}, P_{AS}, or P_{AC}. Despite being possible ion assignments for peak X of the ion trap spectrum, adducts formed from these structures could not be confidently assigned to this spectrum previously due to potential signal overlaps with the $[P_{CS} + Na]^+$ or $[P_{ED} + Na]^+$ adducts. It is also important to note that during analysis of the polymer sample when using the ion trap instrument, the relative abundance readings of peak X are consistent for all spectra produced for this study (which are not

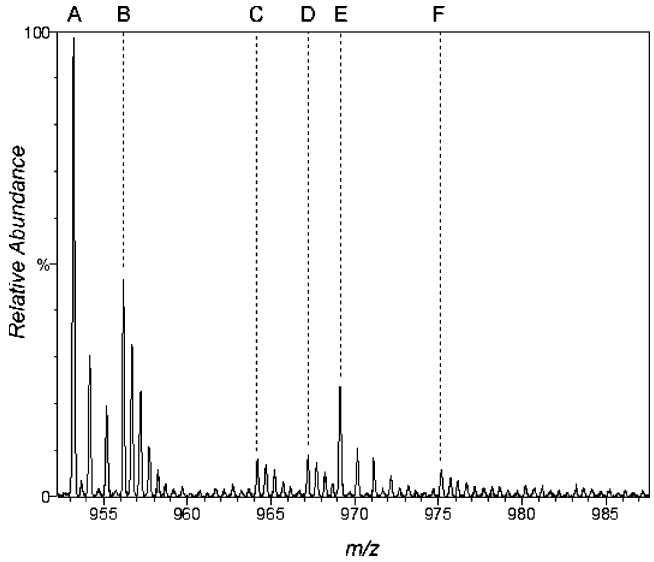

Figure 5. Portion of a spectrum obtained on a Q-TOF Ultima hybrid quadrupole-time-of-flight mass spectrometer from a sample of TRITT mediated polyAA, produced after exposing the polymerizing system to 120 min of ^{60}Co γ-radiation. The peaks that repeat consistently throughout the spectrum are labeled with capital letters.

all shown here). In the TRITT mediated polyNIPAAm system, increased sample storage times led to increased oxidation of polymer species, and thus, increased peak intensities for the oxidized polymer species. The fact that this effect is not observed for peak X in spectra produced from TRITT mediated polyAA suggests that adducts formed from Ox_1P_{ED} contribute to the signal intensity of peak X in a minor manner, if at all. This information, coupled with the observation of peak C in the Q-TOF spectrum, confirms that at least one of the species P_{AS} or P_{AC} is present in the polymer system. Also of note is that no adducts associated with the P_{CS} species are observed in the Q-TOF spectrum, suggesting that the $[P_{CS} + Na]^+$ adduct does not contribute toward peak X of the ion trap spectrum;

Scheme 6. Polymeric Products Identified in Spectra Produced from TRITT Mediated PolyAA Initiated via γ-Radiation in Aqueous Media

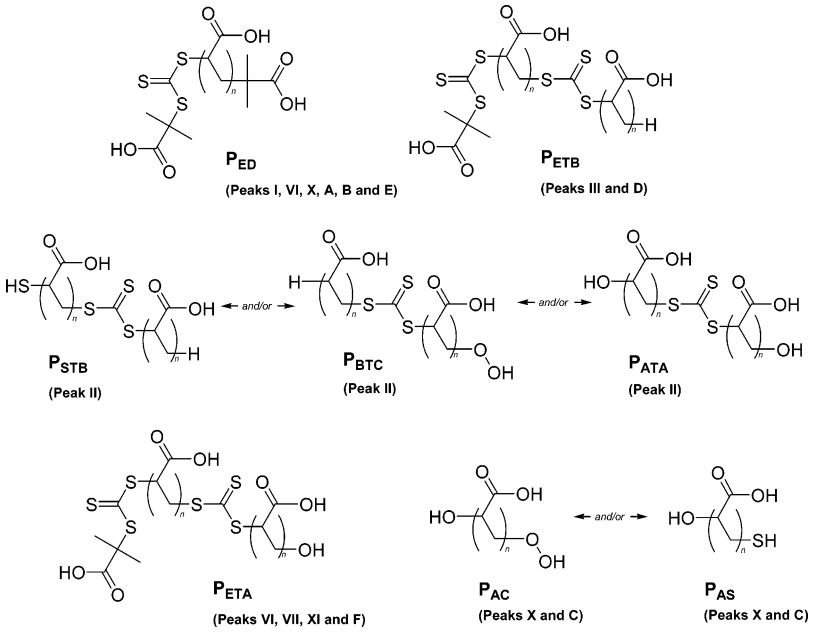

therefore, little evidence supporting the presence of species P_{CS} in the polymer system is found.

Isotopic Peak Pattern Simulations. In a similar manner to the investigations conducted upon polyNIPAAm, isotopic peak pattern simulations were undertaken for polyAA as a final aid to confirm the presence of the structures assigned to the polymer system in the previous mass spectrometry experiments. Such simulations suggest that peak VI of the ion trap spectrum arises predominantly due to the $[P_{ETA} + Na]^+$ and $[P_{ED} + K(KI)]^+$ adducts, whereas for peak X, the presence of the different adduct species assigned to the peaks is equally likely. The interested reader is referred to Figure S3 of the Supporting Information for complete illustrations of the simulations.

The scaled isotopic peak pattern simulations for the final ion assignments have been shown in the upper portion of Figure 4. Excellent agreement is observed between the simulated results and the results obtained experimentally from the ion trap instrument.

End Group Patterns and Mechanistic Implications of Structural Assignments. The polymer end groups observed in the γ-radiation initiated aqueous ambient temperature RAFT polymerizations of NIPAAm and AA are summarized in Scheme 7.

By analyzing the observed end groups, insights into the fundamental radical reactivities and formation processes of the polymerizing systems being investigated are gained. For instance, end groups 1 and 2 confirm that $^{\bullet}$OH and $^{\bullet}$H radicals produced from the radiolysis of water can initiate polymerizations, as indicated by the studies conducted by Acharya et al.[26] The initiating $^{\bullet}$H radicals may also be produced via radiolysis of the RAFT agent or monomer. In addition, end group 3 indicates that $^{\bullet}$OOH species produced from the radiolysis of water also act as radical initiators.

Table 4. Peak Assignments for the Spectrum Obtained from TRITT Mediated PolyAA Shown in Figure 5[51]

peak	ion assignment	normalized abundance	m/z_{exptl}	m/z_{theor}	error (m/z)
A	$[P_{ED} + Na]^+$	1.0	953.19	953.19	0.00
	$[P_{DTD} + Na]^+$			953.19	0.00
B	$[P_{ED} + 2Na]^{2+}$	0.47	956.22	956.22	0.00
	$[P_{DTD} + 2Na]^{2+}$			956.22	0.00
	$[Ox_1P_{ED} + 2K]^{2+}$			964.21	0.00
C	$[P_{AS} + 2K]^{2+}$	0.08	964.21	964.22	0.01
	$[P_{AC} + 2K]^{2+}$			964.23	0.02
D	$[P_{ETB} + 2K]^{2+}$	0.09	967.22	967.16	0.06
E	$[P_{ED} + K]^+$	0.23	969.15	969.16	0.01
	$[P_{DTD} + K]^+$			969.16	0.01
F	$[P_{ETA} + 2Na]^{2+}$	0.06	975.20	975.16	0.04

The initiating capabilities of other radical species associated with the RAFT agent also can be ascertained from an inspection of the identified product structures. End group 4 confirms that the $^{\bullet}$R radicals resulting from the fragmentation of the RAFT agent can initiate polymerizations. Of particular note are the observed product species P_{ETA}, P_{ETB}, and P_{ETC}: trithiocarbonate centered polymer chains capped with end group 5 (see Schemes 2−6 for illustrations of these structures). The trithiocarbonate species within the polymer chains are an expected result of fragmentation occurring on both sides of the symmetrical RAFT agent employed in this study. However, for these structures to form via such a reaction mechanism, the trithiocarbonate end groups in these products must act as initiating species. These structures may also form via radiolysis of trithiocarbonate moieties in polymeric species associated with the core equilibrium of the RAFT process forming initiating trithiocarbonate radical species. Both possible mechanisms indicate that C−S bond cleavage occurs during radiolysis of the controlling RAFT agent, resulting in the formation of initiating trithiocarbonate and $^{\bullet}$R radicals.

Finally, the observed degradation of trithiocarbonate capped chains results in the formation of end group 6 terminated polymers. Polymer chains capped with these end groups potentially form following removal of the polymer samples from the γ-radiation source. However, assuming that the thermal cleavage of C−S bonds observed in the heat treated polyNIPAAm sample is indeed the mode of degradation by which end group 6 capped products form in the untreated samples, the fact that the polymerizing systems are maintained at ambient temperature before and after removal from the γ-radiation source suggests that end group 6 capped species are likely to form during irradiation. Hence, the termination of polymer chains via the degradation of trithiocarbonate end groups plays a role in the

Scheme 7. End Groups Observed in ESI-MS Analyses of TRITT Mediated PolyNIPAAm and PolyAA Produced via γ-Radiation Initiation in Aqueous Environments at Ambient Temperature

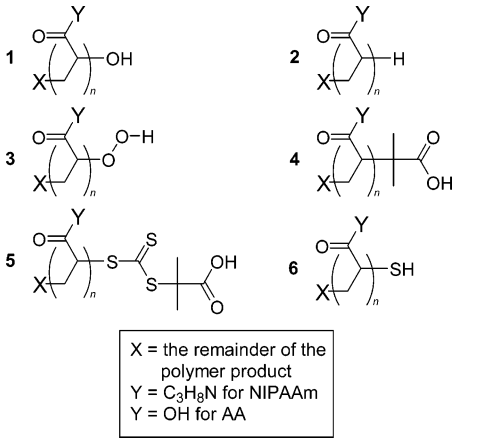

Scheme 8. Summary of the Reactions Involved in γ-Radiation Initiated Aqueous Ambient Temperature RAFT Polymerizations of NIPAAm and AA (When Using a Symmetrical RAFT Agent)

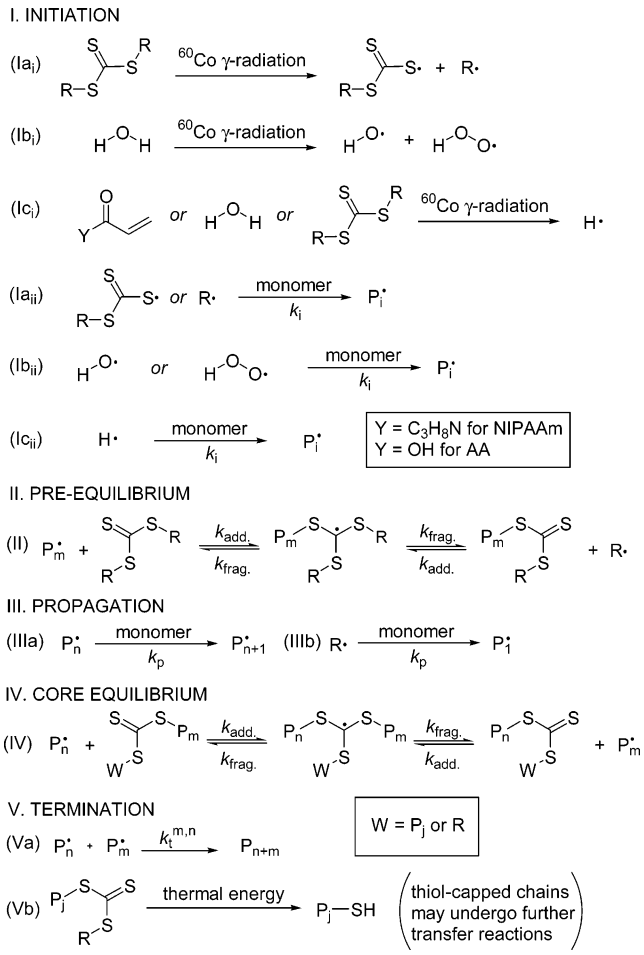

overall mechanistic framework of the polymerizations under investigation.

These insights into the fundamental radical reactivities and polymer formation processes of the systems under study may be incorporated into the widely accepted RAFT process, as shown in Scheme 8. Specifically, the initiation mechanisms incorporate the aforementioned initiating species generated from the radiolysis of water, RAFT agent, and monomer compounds.[27] The initiation of polymer chains from these radical species is illustrated in reactions Ia_{ii}, Ib_{ii}, and Ic_{ii}. During both the pre-equilibrium and the core equilibrium of the RAFT process, fragmentation can occur on both sides of the symmetrical RAFT agent employed in this study, leading to the generation of trithiocarbonate centered polymer chains during the core equilibrium of the RAFT process. Lastly, the termination mechanisms illustrated in reaction V describe combination products (Va) in addition to termination resulting from the degradation of C−S bonds in trithiocarbonate moieties (Vb). As expected, no polymeric product ions indicative of cross-termination reactions were observed.[46]

Conclusion

High-resolution soft ionization mass spectrometry techniques were used to map the product species generated during ambient temperature γ-radiation induced RAFT polymerizations of NIPAAm and AA in aqueous media, allowing for the unambiguous assignment of end groups. Initiating radical species are produced from the radiolysis of water ($^{\bullet}$H, $^{\bullet}$OH, and $^{\bullet}$OOH), the RAFT agent (trithiocarbonate radicals, $^{\bullet}$R and $^{\bullet}$H), and monomer ($^{\bullet}$H), and thus, these radical species contribute toward the generated chain ends. Additionally, evidence of trithiocarbonate end group degradation leading to the formation of thiol terminated chains is presented. In conclusion, comprehensive mapping of the formation pathways and end group patterns of stimuli-responsive polymers was achieved using high-resolution ESI-MS, enabling the design and implementation of these materials to proceed in a more tailored fashion.

Acknowledgment. C.B.-K. thanks the Australian Research Council (ARC) for their financial support in the form of a Discovery Grant as well as an Australian Professorial Fellowship. G.H.-S. acknowledges financial support via an Australian Postgraduate Award (APA). Additionally, we recognize Dr. Leonie Barner and Istvan Jacenyik for their outstanding management of CAMD. T.P.D. acknowledges receipt of a Federation Fellowship. We also thank Prof. Mike Guilhaus and Dr. Russ Pickford at the UNSW Bioanalytical Mass Spectrometry Facility (BMSF) for their many helpful discussions and for the use of the BMSF Q-TOF Ultima hybrid quadrupole-time-of-flight instrument.

Supporting Information Available. Examples of TRITT mediated polyNIPAAm cross-termination products; illustrations of additional chemical structures potentially observed in mass spectra generated from polyNIPAAm and polyAA samples; and illustrations of simulated isotopic peak pattern experiments. This material is available free of charge via the Internet at http://pubs.acs.org.

References and Notes

(1) Chen, S.; Singh, J. *Int. J. Pharm.* **2005**, *295*, 183−190.
(2) Christman, K. L.; Maynard, H. D. *Langmuir* **2005**, *21*, 8389−8393.
(3) Kulkarni, S.; Schilli, C.; Müller, A. H. E.; Hoffman, A. S.; Stayton, P. S. *Bioconjugate Chem.* **2004**, *15*, 747−753.
(4) Lupitskyy, R.; Roiter, Y.; Tsitsilianis, C.; Minko, S. *Langmuir* **2005**, *21*, 8591−8593.
(5) Rauter, H.; Matyushin, V.; Alguel, Y.; Pittner, F.; Schalkhammer, T. *Macromol. Symp.* **2004**, *217*, 109−134.
(6) Chen, J. P.; Hoffman, A. S. *Biomaterials* **1990**, *11*, 631−634.
(7) Hoffman, A. S. *Clin. Chem.* **2000**, *46*, 1478−1486.
(8) Pennadam, S. S.; Lavigne, M. D.; Dutta, C. F.; Firman, K.; Mernagh, D.; Górecki, D. C.; Alexander, C. *J. Am. Chem. Soc.* **2004**, *126*, 13208−13209.
(9) Hoffman, A. S.; Chen, G. *Bioconjugate Chem.* **1993**, *4*, 509−514.
(10) Ding, Z.; Long, C. J.; Hayashi, Y.; Bulmus, E. V.; Hoffman, A. S.; Stayton, P. S. *Bioconjugate Chem.* **1999**, *10*, 395−400.

(11) Stayton, P. S.; Shimoboji, T.; Long, C.; Chilkoti, A. *Nature* **1995**, *378*, 472−474.
(12) Heredia, K. L.; Bontempo, D.; Ly, T.; Byers, J. T.; Halstenberg, S.; Maynard, H. D. *J. Am. Chem. Soc.* **2005**, *127*, 16955−16960.
(13) Liu, J.; Bulmus, V.; Herlambang, D. L.; Barner-Kowollik, C.; Stenzel, M. H.; Davis, T. P. *Angew. Chem., Int. Ed.* **2007**, in press.
(14) Millard, P. E.; Barner, L.; Stenzel, M. H.; Davis, T. P.; Barner-Kowollik, C.; Müller, A. H. E. *Macromol. Rapid Commun.* **2006**, *27*, 821−828.
(15) Bai, R. K.; You, Y. Z.; Pan, C. Y. *Macromol. Rapid Commun.* **2001**, *22*, 315−319.
(16) Barner, L.; Quinn, J. F.; Barner-Kowollik, C.; Vana, P.; Davis, T. P. *Eur. Polym. J.* **2003**, *39*, 449−459.
(17) Barner, L.; Zwaneveld, N.; Perera, S.; Pham, Y.; Davis, T. P. *J. Polym. Sci., Part A: Polym. Chem.* **2002**, *40*, 4180−4192.
(18) Hong, C. Y.; You, Y. Z.; Bai, R. K.; Pan, C. Y.; Borjihan, G. *J. Polym. Sci., Part A: Polym. Chem.* **2001**, *39*, 3934−3939.
(19) Hua, D. B.; Cheng, K.; Bai, R. K.; Lu, W. Q.; Pan, C. Y. *Polym. Int.* **2004**, *53*, 821−823.
(20) Hua, D. B.; Xiao, J. P.; Bai, R. K.; Lu, W. Q.; Pan, C. Y. *Macromol. Chem. Phys.* **2004**, *205*, 1793−1799.
(21) Quinn, J. F.; Barner, L.; Davis, T. P.; Thang, S. H.; Rizzardo, E. *Macromol. Rapid Commun.* **2002**, *23*, 717−721.
(22) Quinn, J. F.; Barner, L.; Rizzardo, E.; Davis, T. P. *J. Polym. Sci., Part A: Polym. Chem.* **2002**, *40*, 19−25.
(23) Zhou, Y.; Zhu, J.; Zhu, X.; Cheng, Z. *Radiat. Phys. Chem.* **2006**, *75*, 485−492.
(24) Hua, D. B.; Zhang, J. X.; Bai, R. K.; Lu, W. Q.; Pan, C. Y. *Macromol. Chem. Phys.* **2004**, *205*, 1125−1130.
(25) Chiefari, J.; Chong, Y. K.; Ercole, F.; Krstina, J.; Jeffery, J.; Le, T. P. T.; Mayadunne, R. T. A.; Meijs, G. F.; Moad, C. L.; Moad, G.; Rizzardo, E.; Thang, S. H. *Macromolecules* **1998**, *31*, 5559−5562.
(26) Acharya, A.; Mohan, H.; Sabharwal, S. *J. Radiat. Res.* **2003**, *44*, 335−343.
(27) Lovestead, T. M.; Hart-Smith, G.; Davis, T. P.; Stenzel, M. H.; Barner-Kowollik, C. *Macromolecules* **2007**, *40*, 4142−4153.
(28) Barner-Kowollik, C.; Davis, T. P.; Stenzel, M. H. *Polymer* **2004**, *45*, 7791−7805.
(29) Hanton, S. D. *Chem. Rev.* **2001**, *101*, 527−569.
(30) Jackson, C. A.; Simonsick, W. J. *Curr. Opin. Solid State Mater. Sci.* **1997**, *2*, 661−667.
(31) Jagtap, R. N.; Ambre, A. H. *Bull. Mater. Sci.* **2005**, *28*, 515−528.
(32) Montando, G.; Carrocia, S.; Montuado, M. S.; Puglisi, C.; Samperi, F. *Macromol. Symp.* **2004**, *218*, 101−112.
(33) Peacock, P. M.; McEwen, C. N. *Anal. Chem.* **2006**, *78*, 3957−3964.
(34) Scrivens, J. H.; Jackson, A. T. *Int. J. Mass Spectrom.* **2000**, *200*, 261−276.
(35) Beyou, E.; Chaumont, P.; Chauvin, F.; Devaux, C.; Zydowicz, N. *Macromolecules* **1998**, *31*, 6828−6835.
(36) Dourges, M. A.; Charleaux, B.; Vairon, J. P.; Blais, J. C.; Bolbach, G.; Tabet, J. C. *Macromolecules* **1999**, *32*, 2495−2502.
(37) Schilli, C.; Lanzendörfer, M. G.; Müller, A. H. E. *Macromolecules* **2002**, *35*, 6819−6827.
(38) Schulte, T.; Siegenthaler, K. O.; Luftmann, H.; Letzel, M.; Studer, A. *Macromolecules* **2005**, *38*, 6833−6840.
(39) Ah Toy, A.; Vana, P.; Davis, T. P.; Barner-Kowollik, C. *Macromolecules* **2004**, *37*, 744−751.
(40) Feldermann, A.; Ah Toy, A.; Davis, T. P.; Stenzel, M. H.; Barner-Kowollik, C. *Polymer* **2005**, *46*, 8448−8457.
(41) Vana, P.; Albertin, L.; Barner, L.; Davis, T. P.; Barner-Kowollik, C. *J. Polym. Sci., Part A: Polym. Chem.* **2002**, *40*, 4032−4037.
(42) Szablan, Z.; Lovestead, T. M.; Davis, T. P.; Stenzel, M. H.; Barner-Kowollik, C. *Macromolecules* **2007**, *40* (1), 26−39.
(43) Lai, J. T.; Filla, D.; Shea, R. *Macromolecules* **2002**, *35*, 6754−6756.
(44) Radical species (C) is formed in the presence of O_2. Small quantities of O_2 are still likely to be present after deoxygenation of the polymer solutions.
(45) Spinks, J. W. T.; Woods, R. J. In *An Introduction to Radiation Chemistry*, 3rd ed.; John Wiley and Sons, Inc.: New York, 1990; pp 255−269.
(46) Feldermann, A.; Coote, M.; Stenzel, M. H.; Davis, T. P.; Barner-Kowollik, C. *J. Am. Chem. Soc.* **2004**, *126*, 15915−15923.
(47) Experimental and theoretical *m*/*z* values have been shown for the peaks contained within the portion of the spectrum illustrated in Figure 2. Abundance readings have been normalized relative to the most abundant peak within this area (peak I).
(48) Llauro, M. F.; Loiseau, J.; Boisson, F.; Delolme, F.; Ladavière, C.; Claverie, J. *J. Polym. Sci., Part A: Polym. Chem.* **2004**, *42*, 5439−5462.
(49) Signal intensities for the spectrum obtained from the heated polymer sample were corrected to take into account the differing signal intensities observed in neat solvent spectra prior to analyzing the respective heated and unheated samples. Because of a potential overlap with peak XVIII, the exact intensity of peak VIII is uncertain; however, the signal intensity of peak VIII must be lower than the 6.7×10^4 au reading observed for the C^{13} isotopomers of peak XVIII.
(50) Experimental and theoretical *m*/*z* values are shown for the peaks contained within the portion of the spectrum shown in Figure 6. Abundance readings are normalized relative to the most abundant peak within this region (peak I).
(51) Abundance readings are normalized relative to the most abundant peak within this region of the spectrum (peak A).

BM700526J